

1 **Human Chorionic Stem Cells: Podocyte Differentiation and Potential for**
2 **the Treatment of Alport Syndrome.**

3

4 Dafni Moschidou¹, Michelangelo Corcelli¹, Kwan-Leong Hau¹, Victoria J
5 Ekwalla¹, Jacques Behmoaras², Paolo De Coppi³, Anna L David¹, George
6 Bou-Gharios⁴, H Terence Cook², Charles D Pusey², Nicholas M Fisk⁵, and
7 Pascale V Guillot^{1*}.

8

9 ¹ University College London, Institute for Women's Health, Maternal and Fetal
10 Medicine Department, London, United Kingdom

11 ² Imperial College London, Faculty of Medicine, Division of Immunity and
12 Inflammation, London, United Kingdom

13 ³ University College London, Institute of Child Health, Stem Cells and
14 Regenerative Medicine Department, London, United Kingdom

15 ⁴ University of Liverpool, Institute of Ageing and Chronic Disease,
16 Musculoskeletal Biology Department, Liverpool, United Kingdom

17 ⁵ University of Queensland, UQ Centre for Clinical Research, Brisbane,
18 Queensland, Australia.

19

20 **running title:** Chorionic Stem Cell Therapy for Alport Syndrome

21

22 * **Corresponding author:** PVG University College London, Institute for
23 Women's Health, Department of Maternal and Fetal Medicine, 86-96 Chenies
24 Mews, London, WC1N 1EH, United Kingdom. Email: p.guillot@ucl.ac.uk,
25 Phone: +44 (0)207 242 9789, Fax: +44 (0)207 404 6181

26

27 **ABSTRACT**

28 Alport syndrome is a hereditary glomerulopathy caused by a mutation in type
29 IV collagen genes, which disrupts glomerular basement membrane, leading to
30 progressive glomerulosclerosis and end-stage renal failure. There is at
31 present no cure for Alport syndrome and cell-based therapies offer promise to
32 improve renal function. Here, we found that human first trimester fetal
33 chorionic stem cells (CSC) are able to migrate to glomeruli and differentiate
34 down the podocyte lineage *in vitro* and *in vivo*. When transplanted into 7-week
35 old Alport 129Sv-*Col4α3^{tm1Dec}/J* (-/-) mice, a single intraperitoneal injection of
36 CSC significantly lowered blood urea and urine proteinuria levels over the
37 ensuing two weeks. In addition, nearly two thirds of transplanted -/- mice
38 maintained their weight above the 80% welfare threshold, with both males and
39 females weighing more than aged-matched non-transplanted -/- mice. This
40 was associated with less renal cortical fibrosis and interstitial inflammation
41 compared to non-transplanted mice, as shown by reduction in murine CD4,
42 CD68 and CD45.2 cells. Transplanted CSC homed to glomeruli, where they
43 expressed *CR1*, *VEGFA*, *SYNAPTOPODIN*, *CD2AP* and *PODOCIN* at the
44 RNA level, and produced both *PODOCIN*, *CD2AP* and *COLIVα3* proteins in
45 non-transplanted -/- mice, ~~suggesting~~ indicating that CSC have adopted a
46 podocyte phenotype. Together, these data indicate that CSC may be used to
47 delay progression of renal pathology via a combination of anti-inflammatory
48 effects and ~~potentially~~ replacement of the defective resident podocytes.

49

50

51

52 INTRODUCTION

53

54 Alport syndrome (AS) is a genetic chronic kidney disease affecting 1 in 5,000
55 individuals. Initially, AS manifests with haematuria, proteinuria and increased
56 blood pressure, with progressive decline in renal function leading to end-stage
57 renal failure requiring replacement therapy. People with AS also suffer from
58 progressive hearing loss, anterior lenticonus, and macular flecks. AS is
59 caused by mutations in the type IV collagen genes encoding the $\alpha3/\alpha4/\alpha5$
60 chains, which are produced exclusively by podocytes [1]. These mutations
61 affect the correct assembly of heterotrimeric CollV $\alpha3/\alpha4/\alpha5$ chains in the
62 glomerular basement membrane (GBM) and result in the GBM failing to
63 mature from the embryonic CollV $\alpha1/\alpha1/\alpha2$ type. Persistence of the immature
64 CollV $\alpha1/\alpha1/\alpha2$ GBM leads to its thickening and splitting, causing progressive
65 tubulointerstitial fibrosis and renal failure [1]. The only current treatment for AS
66 is blockade of the renin-angiotensin system, and proposed treatments include
67 collagen receptor blockade, anti-microRNA therapy, and stem cell therapy [2].
68 The rationale of stem-based therapy is that stem cells isolated from healthy
69 donors will migrate and engraft in renal glomeruli, where they may
70 differentiate into functional podocytes producing new functional GBM. We
71 previously showed that human first trimester fetal blood-derived mesenchymal
72 stem cells (MSC) injected intraperitoneally into fetal mouse recipients
73 migrated to the kidneys where they engrafted in renal glomeruli [3]. However,
74 phenotype rescue by direct cell replacement is challenged by the low level of
75 donor cell engraftment and poor differentiation capacity of the donor cells [4].

76 *Col4 α 3^{tm1Dec}/J* mice are deficient in collagen α 3(IV) chains, and suffer from
77 progressive glomerulosclerosis, with thickening and lamellation of the
78 ~~glomerular basement membrane~~ GBM, segmental glomerular scarring,
79 tubular atrophy, tubulo-interstitial fibrosis and inflammation [5]. The rate of
80 disease progression depends on the genetic background. On a 129Sv
81 background (129Sv-*Col4 α 3^{tm1Dec}/J* mice), inactivation of *col4 α 3* leads to
82 proteinuria by 35 days, elevated blood urea from 50 days onwards, and end
83 stage renal failure by 66 days; whereas on a C57BL/6 background,
84 (C57BL/6-*Col4 α 3^{tm1Dec}/J* mice), these events occur later at 110, 150 and
85 194 days respectively [6].

86

87 We previously showed that whole bone marrow from wild type *Col4 α 3^{+/+}* (+/+) mice
88 transplanted into *Col4 α 3^{-/-}* (-/-) mice produced the missing *CollV α 3*
89 chain, and contributed to improved renal function. However, transplantation of
90 expanded mesenchymal stem cells (MSC) from +/+ mice into -/-mice failed to
91 improve renal function, suggesting either that culture conditions did not
92 maintain cellular plasticity of bone marrow MSC or that other cells, such as
93 hemopoietic stem cells, were involved in restoring renal function [7]. Using a
94 similar model, Sugimoto et al. reported partial restoration of *Col4 α 3* chain
95 expression, as well as improvement of glomerular structure and kidney
96 histology following wild-type bone marrow transplant [8]. Le Bleu et al. also
97 showed that improvement of renal function in *CollV α 3^{-/-}* mice was associated
98 with the expression of the missing α 3 chain of type IV collagen [9]. In all
99 cases the origin of the cells responsible for the improved renal function was
100 not established, but the results suggest that repair of GBM architecture and

101 glomerular integrity is attributable to expression of the collagen type IV α 3
102 chain from podocyte-differentiated donor cells. Using a different AS mouse
103 model, i.e. $\text{CollIV}\alpha 5^{-/-}$ mice, Sedrakyan et al. suggested that mouse stem cells
104 isolated from amniotic fluid delayed interstitial fibrosis and progression of
105 glomerular sclerosis, ameliorating the decline in kidney function [4]. However,
106 donor cells failed to differentiate into podocytes and produce the collagen
107 $\text{IV}\alpha 5$ chain, suggesting that improved renal function may have been achieved
108 via production of anti-inflammatory cytokines.

109 The placenta is a potential source of readily obtainable stem cells throughout
110 pregnancy. We recently isolated and characterized human fetal stem cells
111 derived from first trimester chorion (i.e. chorionic stem cells, CSC)¹⁰. CSC
112 have a spindle-like morphology, are capable of tri-lineage differentiation
113 (osteogenic, adipogenic and chondrogenic) and demonstrate high tissue
114 repair *in vivo* [10]. Over 95% of the cell population lack expression of CD14,
115 CD34 and CD45 but express the mesenchymal markers CD105, CD73,
116 CD44, vimentin, CD29, and CD90, with a subset of cells also expressing the
117 pluripotency markers NANOG, SOX2, cMYC, KLF4, SSEA4, SSEA3, TRA-1-
118 60, and TRA-1-81 and being able to form embryo bodies containing cells from
119 the three germ lineages.

120 In this study, we provide evidence that human CSC can be differentiated
121 down the podocyte lineage *in vitro* and *in vivo*, and delay progression of renal
122 pathology when injected in $\text{CollIV}\alpha 3^{-/-}$ mice, preventing weight loss and
123 decreasing levels of cortical fibrosis and interstitial inflammation.

124

125

126 **MATERIAL AND METHODS**

127

128 **Animals.**

129 Alport (129-*Col4 α 3^{tm1Dec}/J*) mutant (*Col4 α 3^{-/-}*) and wild type (*Col4 α 3^{+/+}*) mice
130 (Jackson Laboratory) were housed in filter cages with a 12:12 hour light-dark
131 cycle (21°C), with water and wet chow (Purina) *ad libitum*, to avoid
132 dehydration which can affect blood urea measurements. Mice were weaned
133 at 30±1 days and culled at 9 weeks of age. All animals were handled in
134 accordance with good animal practice as defined by the British Home Office
135 Animal Welfare Legislation, and animal work was approved by the Institutional
136 Research Ethics Committee (Imperial College London, UK).

137

138 **Glomeruli isolation.**

139 Kidneys from wild type and Alport mice were pushed through a series of
140 sieves (pore sizes 150 μ m, 106 μ m and 45 μ m) using the plunger of a 20 ml
141 syringe. Glomeruli retained on the 45 μ m sieve were collected into a tube and
142 centrifuged at 1000 RPM for 10 minutes.

143

144 **Cell culture.**

145 Collection of surplus human chorionic villi samples was approved by the
146 Research Ethics Committees of Hammersmith & Queen Charlotte's Hospital
147 and of University College London Hospital (UCLH) in compliance with national
148 guidelines (Polkinghorne). CSC were selected by adherence to plastic, further
149 expanded at 10,000 cells/cm² at 37°C in 5% CO² incubator, and studied at
150 passage 4-8. Their fetal origin was confirmed by FISH for X and Y

151 chromosomes on male samples. The cells were fully characterised as
152 previously reported [10], showing the characteristics of stromal MSC-like cells,
153 i.e. capacity to differentiate down the osteogenic, adipogenic and
154 chondrogenic pathway, and expression of CD73, CD90 and CD105. CSC
155 were cultured for three weeks in Dulbecco's modified Eagle's medium-high
156 glucose (Invitrogen) supplemented with 10% fetal bovine serum (BioSera),
157 100 IU/mL penicillin, and 100 µg/mL streptomycin (Invitrogen), i.e. growth
158 medium (D10) on non-coated plastic dishes, or on plastic dishes coated with
159 human type IV collagen (Sigma).

160 Temperature-sensitive conditionally-immortalized human podocyte cell line,
161 derived by Saleem et al. from fresh normal human pediatric kidney
162 specimens, were used as positive controls (gift from Moin Saleem, University
163 of Bristol, Bristol, UK). These cells were originally by incorporating a
164 temperature-sensitive SV40 gene that enables the cells to proliferate at a
165 permissive temperature (33°C) and to differentiate at a non-permissive
166 temperature (37°C), as evidenced by cell morphology and up-regulation of
167 nephrin, synaptopodin, podocin and VEGFA expression [11]. The podocytes
168 were cultured for 21 days at 37°C in 6-well plates in RPMI 1640 medium
169 supplemented with glutamine (Invitrogen, Paisley, UK), 10% fetal calf serum
170 (Biosera, East Sussex, UK), antibiotics and 1% insulin transferrin sodium
171 selenite (Sigma).

172

173 **Fluorescence immunostaining and confocal microscopy.**

174 CSC were grown exponentially on 10-mm coverslips before being fixed in 4%
175 PFA, 250 mM HEPES (pH 7.6; 10 min, 4°C), re-fixed in 8% PFA, 250 mM

176 HEPES (pH 7.6; 50 min, 4°C) and rinsed 3X with PBS. After fixation, the cells
177 were incubated (30 min) with 20 mM glycine in PBS, blocked (1 h) with PBS+
178 (PBS supplemented with 1% BSA, 0.2% fish skin gelatin, 0.1% casein; pH
179 7.6), incubated (2 h) with Anti- NHPS2 or Podocin (Sigma, 1:1,000) in PBS+,
180 washed (5X over 1.5 h) in PBS+, incubated (1 h) with secondary antibodies
181 (Alexa 488 goat anti rabbit) in PBS+, rinsed (overnight, 4°C) in PBS+, and
182 mounted in VectaShield labelled with DAPI (Vector Labs). Fluorescence
183 confocal laser scanning microscopy images were collected on a Leica TCS
184 SP5 (X400 PL APO oil objective) and transferred to Adobe Photoshop (Adobe
185 Systems).

186

187 **Chemotaxis assay.**

188 CSC suspension (100 μ l of 10^7 cells/ml in DMEM-0.5% BSA) was placed in
189 the upper compartment of a chemotaxis chamber. Chemoattractants
190 (glomeruli from +/+ or -/- mice, or DMEM-0.5% BSA) were placed in the lower
191 compartment, separated by a 8 μ m polycarbonate filter (Neuroprobe). The
192 cells were allowed to undergo chemotaxis (1 hour). The filter was then
193 removed, washed, fixed and stained (1% hematoxylin) (Sigma). Ten random
194 fields were counted at X40 magnification by a blinded observer (triplicates).
195 The migration index (MI) was calculated as the ratio of the number of cells
196 migrating towards the chemoattractant to the number of cells migrating
197 towards media alone.

198

199 **Cell transplantation.**

200 Cells (10^6 in 10 μ l PBS, pooled from 5 different donors to reduce inter-donor
201 differences) were injected intraperitoneally in 7 week-old *Col4a3^{-/-}* (-/-) or wild
202 *Col4a3^{+/+}* (+/+) (n=25 per group). Animal weight was recorded 3 times per
203 week and mice were culled 2 weeks after transplantation or when weight loss
204 exceeded 20% of the maximum previously achieved weight, as mandated by
205 the British Home Office.

206

207 **Quantitative real time RT-PCR (QRT-PCR).**

208 Total RNA (n=8 mice per group) was extracted from the glomeruli using
209 TRIzol (Invitrogen) and cDNA synthesized using random primers and 1 μ l of
210 200 U M-MLV Reverse Transcriptase in the presence of dNTPs (Promega
211 Corp.) (10 min, 75°C; 120 min, 42°C and 10 min, 75°C). QRT-PCR was
212 performed with the ABI Step-One Plus Sequence Detector (Applied
213 Biosystems). We used primers amplifying sequences of the β -actin gene
214 (accession number: NM_001101) present in humans but not in mice to
215 determine the amount of human cellular cDNA in samples (primer specificity
216 confirmed by absence of amplification of mouse cDNA), and primers common
217 to both human and mouse to determine the total cDNA in each sample, as
218 previously described [12]. For both sets, the absence of dimer formation was
219 confirmed using Dissociation Curves 1.0 software (Applied Biosystems).
220 Human:mouse chimerism was estimated as a ratio. Serial dilution of human
221 cDNA in mouse cells formed the calibration curves. The primer sequences are
222 shown in Table 1.

223

224 **Histology.**

225 Fresh kidneys (n=6 mice) were fixed in Bouin's fixative (Sigma) for 4 hours,
226 dehydrated using serial dilutions of ethanol, embedded in wax, sectioned and
227 stained with Picrosirius red stain. Five random non-overlapping fields were
228 assessed at X200 magnification by a blinded observer, under polarised or
229 white light with an Olympus BX51 microscope.

230

231 **Immunohistology.**

232 Fresh kidneys were removed and fixed in a solution containing 1% PFA,
233 0.075M L-Lysine, 0.01M Sodium Periodate and 0.037M Phosphate buffer (all
234 reagents from Sigma) for 4 hours at 4°C. Tissues were then stored overnight
235 into 7% sucrose in PBS (Sigma) at 4°C, immersed in OCT compound (VWR)
236 and snap frozen before being stored at -80°C for further analysis. For
237 immunofluorescence, 4 µm sections were air dried (2 hours), fixed in acetone
238 (10 min, 4°C), air dried for a further 2 hours and denatured (1 hour, 4°C) using
239 a solution of 6M Urea and 0.1M Glycine in PBS (pH 3.5, all reagents from
240 Sigma). Slides were then washed with PBS and incubated overnight at 4°C
241 with a Col4a3 primary antibody diluted 1:2000 in 7% non-fat dry milk. The
242 Col4a3 antibody (kindly donated by Dr Dominic Cosgrove, Boys Town
243 National Research Hospital, Omaha, NE) is an affinity purified rabbit
244 polyclonal antibody raised against a peptide mapping the NC1 region of
245 collagen α3 Type IV. This antibody has been tested for cross-reactivity by the
246 provider and reacts with human and mouse [14]. The presence of donor cells
247 was visualised using a rabbit monoclonal antibody raised against human
248 vimentin (Abcam ab137867). Slides were then washed in PBS, incubated at
249 room temperature for 1 hour with a FITC-conjugated secondary antibody,

250 washed with PBS and mounted with Vectashield containing DAPI (Vector
251 Laboratories, Peterborough, UK) for visualisation using a confocal laser-
252 scanning microscope Leica TCS SP5 (x1000 PL APO oil objective; Leica,
253 Wetzlar, Germany).

254

255 **Immunohistochemistry.**

256 Immunoperoxidase staining for the ~~macrophage/monocyte~~ T-helper cell
257 marker CD4 (BD Biosciences), the leucocyte marker CD45.2 (eBiosciences)
258 and the macrophage marker CD68 (Abcam) was performed on PLP-fixed
259 kidney cryostat sections (4µm). Sections were incubated overnight at 4°C with
260 primary antibody. For the biotin-conjugated CD45.2 antibody, endogenous
261 biotin and avidin were blocked prior to the addition of the primary antibody,
262 using biotin and avidin block solutions respectively (Vector Labs). Sections
263 were then washed with PBS, incubated with the appropriate HRP-conjugated
264 secondary antibody (Golden Bridge International), washed with PBS and
265 visualised using DAB. The sections were then counterstained with
266 hematoxylin, dehydrated and mounted using DPX (Sigma).

267

268 **Blood urea analysis.**

269 Blood samples were centrifuged at 1,300 g (10 min, 4°C) and the supernatant
270 was stored at -80°C until analysis. Urea was measured using a urea/ammonia
271 detection kit (R-Biopharm), according to the manufacturers instructions. All
272 samples were analysed at the same time to avoid batch variation.

273

274 **Measurement of proteinuria/hematuria.**

275 Urine was collected from 9 week-old mice and proteinuria was quantitatively
276 measured using mouse albumin and creatinine ELISA (albumin urinary level /
277 creatinine urinary level) (Exocell), according to the manufacturers instructions.
278 ~~assessed for the presence of protein or erythrocytes by dipstick analysis~~
279 ~~(Siemens Healthcare, Surrey, UK). Results were based on color change and~~
280 ~~ranged from 0/trace to + + + +, according to the manufacturer's detection guide.~~
281 ~~Controls included +/+ non-transplanted mice (negative control) and -/- non-~~
282 ~~transplanted mice (positive control).~~ Analysis was performed by two
283 observers blinded as to whether each sample was from transplanted or non-
284 transplanted -/- or +/+ groups.

285

286 **Western Blotting.**

287 Total protein was extracted using RIPA buffer containing protease inhibitor
288 cocktail and PMSF (Sigma). Protein concentrations were determined using
289 the BCA assay (Thermo-Scientific) with BSA as standard. Proteins were run
290 on 8% SDS-PAGE, transferred to nitrocellulose membranes, blocked with milk
291 and incubated with primary antibodies for human-specific COL1A3 (160-190
292 kDa), PODOCIN (42 kDa, Santa Cruz) and CD2AP (71 kDa, Millipore).
293 Membranes were incubated with secondary HRP-conjugated anti-goat IgG
294 (Santa Cruz) and proteins detected using enhanced chemiluminescence
295 (Thermo-Scientific). GAPDH was used as a loading control (Millipore).

296

297 **Statistical analysis.**

298 Data are expressed as mean±SEM (standard error) or median and range.
299 Parametric and non-parametric statistics were applied after testing
300 distributions on histograms. P < 0.05 was considered significant.

301

302

303 RESULTS

304

305 **CSC cultured on human type IV collagen or co-cultured with glomeruli** 306 **express podocyte markers and migrate to glomeruli *in vitro*.**

307 CSC were cultured for three weeks in growth medium (D10), either on non-
308 coated plastic dishes, on plastic dishes coated with human collagen IV (CSC
309 on COLIV). Alternatively, CSC were co-cultured without cell contact, with
310 freshly-isolated COL4 α 3^{-/-} and COL4 α 3^{+/+} glomeruli (CSC-glomeruli co-
311 culture). After 3 weeks of culture, the expression level of various podocyte
312 markers was analysed by QRT-PCR (**Figure 1A**). The podocyte line
313 expressed *NEP HRIN*, a gene involved in renal filtration; *PODOCIN*,
314 expression of which is restricted to mature podocytes; *VEGFA*, produced
315 during kidney morphogenesis to guide endothelial cells towards glomeruli;
316 *SYNAPTOPODIN*, an actin-associated gene; *CD2AP*, which **regulates the**
317 **translocation of dendrin to reorganize podocyte cytoskeleton and stabilize the**
318 **slit diaphragm**; and CR1, complement receptor 1 which protects podocytes
319 from complement attack. The expression of these genes was almost
320 undetectable in CSC cultured alone in growth medium on non-coated dishes.
321 In contrast, the expression of all markers was upregulated when CSC were
322 cultured on dishes coated with human collagen IV. Expression of *NEPHRIN*,

323 *SYNAPTOPODIN*, and *CR1* was further up-regulated when the cells were co-
324 cultured with *-/-* glomeruli, although *PODOCIN* expression was lower. The
325 expression levels of *VIMENTIN* and *FIBRONECTIN* remained unchanged in
326 CSC cultured on Collagen Type IV or by co-culture with glomeruli (data not
327 shown). Confocal immunofluorescence showed that CSC cultured for 3 weeks
328 on human type IV collagen or co-cultured with *-/-* glomeruli expressed
329 *PODOCIN* at a protein level (**Figure 1B**). These data indicate that CSC have
330 the potential to differentiate down the podocyte lineage. Next, we used a
331 chemotaxis assay where CSC were allowed to migrate for 1h towards freshly
332 isolated *Col4a3^{-/-}* (*-/-*) or *Col4a3^{+/+}* (*+/+*) glomeruli *ex vivo*. CSC did not
333 passively migrate towards growth medium (GM) alone, but showed high
334 chemotaxis towards *+/+* glomeruli and significantly greater chemotaxis
335 towards *-/-* glomeruli (9.5 ± 1.5 MI vs. 21.1 ± 2.6 MI respectively) (**Figure 1C**).
336 These results indicate that *-/-* glomeruli produce soluble factors that may
337 stimulate migration and differentiation of CSC, and rationalize the use of CSC
338 for the treatment of AS.

339

340 **CSC transplanted into *-/-* mice engrafted into glomeruli, expressed**
341 **podocyte markers, and produce *PODOCIN* and the missing *Col4 α 3***
342 **protein.**

343 We injected 10^6 CSC intraperitoneally into 7 week old *-/-* and *+/+* mice and
344 assessed the fate of donor cells 2 weeks later. CSC injection was performed
345 at 7 weeks postnatally because analysis of the disease history in *-/-* mice
346 revealed the presence of blood and protein in urine at this age, whereas the
347 levels of blood urea, which is a robust measure of renal function in mice, was

348 still comparable to the values found in +/+ mice. Donor cell engraftment in
349 isolated glomeruli was determined by QRT-PCR using human-specific and
350 non-specific primers for the housekeeping gene β -actin, as previously
351 described¹³. Results showed that transplanted CSC homed to glomeruli, with
352 10.8 fold higher engraftment in -/- (n=8) compared to +/+ glomeruli (n=8)
353 (**Figure 2A**). Using human-specific antibody against vimentin protein,
354 histological analysis of kidney sections from transplanted and non-
355 transplanted -/- mice revealed the presence of donor CSC in glomeruli, with
356 some donor cells being also visible outside the glomeruli of CSC-
357 transplanted -/- mice (**Figure 2B**). Engrafted CSC expressed the podocyte
358 markers *CR1*, *VEGFA*, *SYNAPTOPODIN* and *CD2AP* (**Figure 2C**). Human-
359 specificity of the primers was verified using RNA from kidneys of -/- non-
360 transplanted mice, which showed absence of amplification. At the protein
361 level, engrafted CSC produced *PODOCIN*, *CD2AP* and *COL4A3*, which are
362 absent in non-transplanted -/- and +/+ mice (**Figure 2D and 2E**).

363

364 **Improvement of the -/- phenotype.**

365 Non-transplanted -/- mice (n=25) progressively lost weight between 7 and 10
366 weeks. By 9 weeks of age, 63% mice dropped their weight below the 20%
367 endpoint level mandated by the British Home Office and had to be culled. In
368 contrast, all CSC-transplanted -/- mice (n=48) maintained their weight until 9
369 weeks (**Figure 3A**), at which age both transplanted -/- males and females
370 were heavier than age- and sex-matched non-transplanted -/- mice, with their
371 weight being similar to wild-type +/+ mice (**Figure 3B**).

372 Next, we measured blood urea in non-transplanted +/+ and -/- mice over 90
373 days. Levels remained under 20 mmol/l until day 90 in +/+ mice (**upper panel**
374 **of Figure 3C**, red dots, n=41), whilst all -/- mice showed elevated blood urea
375 levels by 58 days of age (**lower panel of Figure 3C**, blue dots, n=45). In
376 contrast, urea levels were lower in 9 week-old -/- mice transplanted with CSC
377 two weeks before than in non-transplanted -/- mice (18.8 ± 2.0 mmol/L, n=25
378 vs. 29.9 ± 0.7 mmol/L, n=10; mean \pm SEM, $P < 0.01$), with 64% of transplanted -/-
379 mice showing levels similar to +/+ mice (**Figure 3D**). ~~However, despite~~
380 ~~transplantation of CSC being associated with lower blood urea levels,~~
381 ~~proteinuria and hematuria, which were already elevated in -/- mice at the time~~
382 ~~of cell therapy, remained unchanged following CSC transplantation (data not~~
383 ~~shown).~~ Quantification of urine proteinuria (albumin / creatinine level) revealed
384 a significant reduction in -/- mice transplanted with CSC compared to their
385 non-transplanted counterparts (35.6 ± 1.8 , n=21 vs. 47.5 ± 3.2 , n=16;
386 mean \pm SEM, $P < 0.01$) (**Figure 3E**).

387

388 **CSC transplantation lowered tubulointerstitial fibrosis and reversed**
389 **cortical inflammation.**

390 We next measured tubulointerstitial fibrosis within the cortex using Picrosirius
391 red staining (PSR). PSR in kidneys from CSC-transplanted -/- mice was lower
392 than levels found in non-transplanted -/- mice (0.089 ± 0.0018 , n=6 vs.
393 0.040 ± 0.0015 , n=6, $P < 0.001$), indicating a decrease in tubulointerstitial
394 fibrosis (**Figure 4A and 4B**). Quantification of renal inflammation showed that
395 CSC transplantation reduced the number of glomerular T-helper cells (anti-
396 CD4), macrophages (anti-CD68), and haematopoietic cells (anti CD45.2) in -/-

397 mice indicating a marked decreased in cortical inflammation (**Figure 4C and**
398 **4D**).

399

400 **Col4a3 mutation down-regulated endogenous murine podocyte gene**
401 **expression, and CSC transplantation partially restored renal mRNA**
402 **expression levels.**

403 We next assessed whether the presence of exogenous cells modified gene
404 expression of resident podocytes. Results showed that expression of murine
405 *Nephrin*, *Podocin*, *Synaptopodin*, *Cd2ap*, *Cr1* and *Vegfa* was higher in the
406 glomeruli of non-transplanted +/+ mice compared to non-transplanted -/- mice
407 (**Figure 5**). However, CSC transplantation upregulated the renal mRNA
408 expression of *Nephrin*, *Podocin*, *Synaptopodin*, *Cd2ap* and *Vgfa*, suggesting
409 that the decrease in glomerular inflammation in transplanted mice was
410 associated with restored podocyte activity.

411

412

413 **DISCUSSION**

414

415 Several studies have suggested that renal pathology in models of AS can be
416 improved by cell therapy, although the mechanisms mediating these effects
417 remain elusive, with conflicting results possibly attributable to variations in
418 donor cell types. It is therefore essential to identify easily accessible sources
419 of stem cells with high therapeutic potential for the treatment of AS [14]. In this
420 study, we used human first trimester fetal chorionic stem cells (CSC), which
421 are isolated from chorionic villi sampling in ongoing pregnancies and can be

422 expanded to high numbers *ex vivo*, while maintaining tissue repair potential¹⁰.
423 For example, when transplanted into collagen type I-deficient mice, they
424 reduced fracture rate and increased bone plasticity; and accelerated skin
425 wound healing [10, 15].

426

427 *Col4α3^{-/-}* mice are a model of severe human Alport syndrome. At 7 week of
428 age, *-/-* Alport mice show high levels of proteinuria, but normal weight and
429 blood urea. Over the next two weeks, blood urea rapidly increases, whilst
430 body weight drops and mice show pronounced interstitial fibrosis and
431 macrophage infiltration. We investigated the capacity of CSC to prevent
432 glomerulopathy in 129Sv-*Col4α3^{-/-}* mice. We show that 9 week-old *-/-* mice
433 transplanted with CSC two weeks before have significantly lower blood urea
434 and urine proteinuria, compared to their non-transplanted counterparts.
435 Although animal welfare restrictions prevented us from studying the clinical
436 endpoint of survival, all transplanted *-/-* mice maintained their weight until 9
437 week of age. This is important because improvement in renal histology is not
438 necessarily associated with delay in death from renal failure [16]. However,
439 the genetic background of the Alport mice has a strong effect on the rate of
440 disease progression [17]. Contrary to 129Sv-*Col4α3^{tm1Dec}/J (-/-)* mice, which
441 progressively lose weight and do not survive beyond 10 weeks of age, the
442 survival time of homozygous mutant mice is extended to about 14 weeks of
443 age in mice maintained on a mixed genetic background or to 25-30 weeks on
444 the C57BL/6j background. Consequently, we suggest that the elevated blood
445 urea and 20% weight loss we report may be considered as surrogates for
446 end-stage renal failure. ~~We found that proteinuria, which was already elevated~~

447 ~~at the time of cell injection, did not return to normal levels but did not increase~~
448 ~~further in transplanted -/- mice, whilst it increased in non-transplanted -/- mice~~
449 ~~. This was not surprising, since structural damage to the GBM would be~~
450 ~~unlikely to be reversed within 2 weeks.~~

451

452 Increasing evidence from stem cell transplantation in acquired injury models
453 points to the well characterised anti-inflammatory actions of exogenous stem
454 cells making a major contribution to therapeutic results. For example, murine
455 amniotic fluid cells transplanted into *Col4 α 5^{-/-}* mice before the onset of
456 proteinuria have been reported to modify the course of renal fibrosis, despite
457 donor cells failing to differentiate into podocytes or produce collagen IV α 5⁴.
458 Here, we found reduced renal fibrosis and cortical inflammation in
459 transplanted mice, which may reflect the anti-inflammatory effect of donor
460 cells or the replacement of defective renal cells. We also found that CSC
461 migrated to the glomeruli, where they persisted over 2 weeks and expressed
462 *CR1*, *VEGFA*, *SYNAPTOPODIN*, *CD2AP* and *PODOCIN* at the gene level,
463 and produced *PODOCIN*, *CD2AP* and *COLIV α 3* proteins. ~~which are missing~~
464 ~~in non-transplanted -/- mice~~. These data indicate that transplanted CSC have
465 adopted a podocyte phenotype. However, focal staining for *Col4a3* in the
466 kidneys does not prove true GBM deposition, and it will be necessary to
467 demonstrate assembly of the correct collagen type IV in the GBM to
468 investigate whether the *Col4a3* produced by CSC co-assemble with *Col4a4*
469 and *Col4a5* to improve GBM structure [18]. Similarly to our findings, LeBleu et
470 al. found that wild-type bone marrow-derived cells transplanted into *Col4 α 3* *-/-*
471 mice improved renal histology and function, with donor cells differentiating into

472 VEGF and collagen IV-expressing podocytes [9]; and a recent study by Lin et
473 al. demonstrates that secretion of $\alpha3\alpha4\alpha5$ (IV) heterotrimers is sufficient to
474 slow disease progression by partially restoring the defective collagen network
475 [19].

476

477 Interestingly, we also found that CSC transplantation stimulated resident
478 podocyte activity, suggesting that the production of Col4 α 3 from donor cells
479 act as a feed-back to modulate podocyte activity, possibly by releasing trophic
480 factors that promote the differentiation and regeneration of endogenous
481 podocyte progenitors to differentiate into mature podocytes. Although
482 endogenous podocytes remain unable to express the correct form of Collagen
483 type IV, stimulation of podocyte progenitors differentiation into podocytes by
484 donor stem cells may contribute to the amelioration of filtration function [20].

485 Although it is often assumed that the presence of exogenous cells at the site
486 of injury and their differentiation into target cell phenotypes accounts for the
487 therapeutic effects observed, there is still a lack of evidence for the causality
488 between the two. An increasing number of studies challenge the concept of
489 donor cells acting as a building blocks to replace damaged endogenous cells
490 and data suggest that beyond their potential as a source of cell replacement,
491 stem cells also mediate paracrine treatment. In addition, data suggest that
492 donor cells influence the complex cross-talk between resident cells and
493 extracellular matrix. It is possible that exogenous stem cells reprogramme
494 resident macrophages from an anti-inflammatory to a pro-inflammatory
495 phenotype, as is the case in sepsis [21]. This mechanism might account for
496 the therapeutic effects of wild type bone marrow that we previously reported⁷.

497 For example, blockade of tumour necrosis factor-alpha (TNF- α), a pro-
498 inflammatory cytokine, has been shown to ameliorate glomerulosclerosis and
499 proteinuria in AS mice [22].

500 We believe that CSC may have strong potential for the treatment of
501 glomerulopathies and further studies are indicated to establish the precise
502 mechanism of action of these cells in treatment of AS.

503

504

505 **ACKNOWLEDGEMENT:**

506 This research was funded by Kidney Research UK, Genzyme Renal
507 Innovations Programme and by the National Institute for Health Research
508 Biomedical Research Centre at Great Ormond Street Hospital for Children
509 NHS Foundation Trust and University College London. ALD is funded by
510 Department of Health through NIHR UCL/UCLH Biomedical Research Centre.
511 We acknowledge support from NIHR Imperial Biomedical Research Centre.

512

513

514 **AUTHOR DISCLOSURE STATEMENT:**

515 No competing financial interests exist.

516

517 ~~**AUTHORS CONTRIBUTION:**~~

518 ~~DM, MC, KLH, VE, PES, JB: Collection and/or assembly of data, data~~
519 ~~analysis and interpretation; GBG, GDP, ALD, PDC, HTC: Conception and~~
520 ~~design, financial support, manuscript editing; ALD, PDC, NMF: Provision of~~
521 ~~study material; NMF: data analysis and interpretation, manuscript writing;~~

522 ~~PVG: Conception and design, data analysis and interpretation, financial~~

523 ~~support, manuscript writing.~~

524

525 **REFERENCES**

526

- 527 1. Abrahamson DR, Prettyman AC, Robert B and St John PL. (2003).
528 Laminin-1 reexpression in Alport mouse glomerular basement
529 membranes. *Kidney Int* 63:826-834.
- 530 2. Gross O, Perin L and Deltas C. (2014). Alport syndrome from bench to
531 bedside: the potential of current treatment beyond RAAS blockade and
532 the horizon of future therapies. *Nephrol Dial Transplant* 29:iv124-iv130.
- 533 3. Guillot PV, Cook TH, Pusey CD, Fisk NM, Harten S, Moss J, Shore I,
534 and Bou-Gharios G. (2008). Transplantation of human fetal
535 mesenchymal stem cells improves glomerulopathy in a collagen type I
536 alpha 2-deficient mouse. *J Pathology* 214(5):627-636.
- 537 4. Sedrakyan S, Da Sacco S, Milanese , Shiri L, Petrosyan A, Varimezova
538 R, Warburton D, Lemley KV, De Filippo RE and Perin L. (2012).
539 Injection of amniotic fluid stem cells delays progression of renal
540 fibrosis. *J Am Soc Nephrol* 23:661-673.
- 541 5. Miner JH and Sanes JR. (1996). Molecular and functional defects in
542 kidneys of mice lacking collagen alpha 3(IV): implications for Alport
543 syndrome. *J Cell Biol* 135:1403-1413.
- 544 6. Andrews KL, Mudd JL, Li C and Miner JH. (2002). Quantitative trait loci
545 influence renal disease progression in a mouse model of Alport
546 syndrome. *Am J Pathol* 160:721-730.
- 547 7. Prodromidi EI, Poulson R, Jeffery R, Roufosse CA, Pollard PJ, Pusey
548 CD and Cook HT. (2006). Bone marrow derived cells contribute to

- 549 podocyte regeneration and amelioration of renal disease in a mouse
550 model of Alport Syndrome. *Stem Cells* 24:2448-2455.
- 551 8. Sugimoto H, Mundel TM, Sund M, Xie L, Cosgrove D and Kalluri R.
552 (2006). Bone-marrow-derived stem cells repair basement membrane
553 collagen defects and reverse genetic kidney disease. *Proc Natl Acad*
554 *Sci (USA)* 103:7321-7326.
- 555 9. LeBleu V, Sugimoto H, Mundel TM, Gerami-Naini B, Finan E, Miller
556 CA, Gattone VH 2nd, Shield CF 3rd, Folkman J and Kalluri R. (2009).
557 Stem cell therapies benefit Alport syndrome. *J Am Soc Nephrol*
558 20:2359-2370.
- 559 10. Jones GN, Moschidou D, Puga-Iglesias TI, Kuleszewicz K, Vanleene
560 M, Shefelbine SJ, Bou-Gharios G, Fisk NM, David AL, De Coppi P and
561 Guillot PV. (2012). Ontological differences in first compared to third
562 trimester human fetal placental chorionic stem cells. *PLoS One*
563 7:e43395.
- 564 11. Saleem MA, O'Hare MJ, Reiser J, Coward RJ, Inward CD, Farren T,
565 Xing CY, Ni L, Mathieson PW and Mundel P. (2002). A conditionally
566 immortalized human podocyte cell line demonstrating nephrin and
567 podocin expression. *J Am Soc Nephrol* 13:630–638.
- 568 12. Guillot PV, Abass O, Bassett JH, Shefelbine SJ, Bou-Gharios G, Chan
569 J, Kurata H, Williams GR, Polak J and Fisk NM. (2008). Intrauterine
570 transplantation of human fetal mesenchymal stem cells reduces bone
571 pathology in osteogenesis imperfecta mice. *Blood* 111:1717-1725.

- 572 13. Miner, JH and JR Sanes. (1994). Collagen IV $\alpha 3$, $\alpha 4$, and $\alpha 5$ chains in
573 rodent basal lamina: Sequence, distribution, association with laminins,
574 and developmental switches. *J. Cell Biol.* 127: 879-891.
- 575 14. Wong C and Rogers I. (2009). Cell therapy for Alport syndrome. *J Am*
576 *Soc Nephrol* 20:2279-2281.
- 577 15. Jones GN, Moschidou D, Abdulrazzak H, Kalirai BS, Vanleene M,
578 Osatis S, Shefelbine, SJ, Horwood NJ, Marenzana M, De Coppi P,
579 Bassett JH, Williams GR, Fisk NM and Guillot PV. (2014). Potential of
580 human fetal chorionic stem cells for the threatment of osteogenesis
581 imperfecta. *Stem Cells Dev* 23:262-276.
- 582 16. Ninichuk V, Gross O, Segerer S, Hoffmann R, Radomska E,
583 Buchstaller A, Huss R, Akis N, Schlondorff D and Anders HJ. (2006).
584 Multipotent mesenchymal stem cells reduce interstitial fibrosis but do
585 not delay progression of chronic kidney disease in collagen4A3-
586 deficient mice. *Kidney Int* 70:121-129.
- 587 17. Cosgrove D, Meehan DT, Grunkemeyer JA, Kornak JM, Sayers R,
588 Hunter WJ and Samuelson GC. (1996). Collagen COL4A3 knockout: a
589 mouse model for autosomal Alport syndrome. *Genes Dev* 10:2981-
590 2992.
- 591 18. Gross O, Borza DB, Anders HJ, Licht C, Weber M, Segerer S, Torra R,
592 Gubler MC, Heidet L, Harvey S, Cosgrove D, Lees G, Kashtan C,
593 Gregory M, Savige J, Ding J, Thorner P, Abrahamson DR, Antignac C,
594 Tryggvason K, Hudson B, Miner JH. (2009). Stem cell therapy for
595 Alport syndrome: the hope beyond the hype. *Nephrol Dial Transplant*
596 24:731-734.

- 597 19. Lin X, Suh JH, Go G and Miner JF. (2014). Feasibility of repairing
598 glomerular basement membrane defects in Alport syndrome. *J Am Soc*
599 *Nephrol* 25:687-692.
- 600 20. Lasagni L, Angelotti ML, Ronconi E, Lombardi D, Nardi S, Peired A,
601 Becherucci F, Mazzinghi B, Sisti A, Romoli S, Burger A, Schaefer B,
602 Buccoliero A, Lazzeri E and Romagnani P. (2015). Podocyte
603 regeneration driven by renal progenitors determines glomerular
604 disease remission and can be pharmacologically enhanced. *Stem Cell*
605 *Reports* 5:248-263.
- 606 21. Tyndall A and Pistoia V. (2009). Mesenchymal stem cells combat
607 sepsis. *Nat Med* 15:109-118.
- 608 22. Ryu M, Mulay SR, Miosge N, Gross O and Anders HJ. (2012). Tumour
609 necrosis factor- α drives Alport glomerulosclerosis in mice by promoting
610 podocyte apoptosis. *J Pathol* 226(1):120-131.

611
612
613
614
615
616
617
618
619
620
621

622 **FIGURE LEGENDS**

623 **Figure 1 | CSC cultured in permissive conditions express podocyte**
624 **markers and migrate to glomeruli *in vitro*. A.** Quantitative real-time RT-
625 PCR **using human-specific primers** and showing expression of the podocyte
626 markers NEPHRIN, SYNAPTOPODIN, PODOCIN, CD2AP, VEGFA, and CR1
627 in a temperature-inducible differentiated podocyte cell line (grey bars), **in**
628 **mouse glomerular cells (black bars)**, in CSC cultured for three weeks either in
629 growth medium (D10) on non-coated plastic dishes (green bars), on plastic
630 dishes coated with human collagen IV (blue bars), and in CSC co-cultured
631 with **-/- glomeruli (red bars) and +/+ glomeruli (white bars)**. Values are
632 expressed as $2^{-\Delta CT}$, with $\Delta CT = \beta\text{-actin} - \text{gene of interest}$. *** $P < 0.01$ $n = 3$
633 samples per group, error bars are SEM. **B.** Confocal immuno-fluorescence of
634 CSC cultured for three weeks on human Type IV collagen **and co-cultured**
635 **with -/- glomeruli**. Anti-podocin marker was stained with FITC (green), and
636 nuclei with DAPI (blue). X10 magnifications. **C.** *In vitro* chemotaxis assay
637 where CSC were allowed to migrate towards +/+ (clear bars) or -/- (red bars)
638 freshly isolated glomeruli for 1 hour. *** $P < 0.01$, $n = 3$ per group, error bars are
639 SEM.

640

641 **Figure 2 | Transplanted CSC engrafted into -/- glomeruli and expressed**
642 **podocyte markers. A.** Quantitative real-time RT-PCR showing expression of
643 β -actin using human-specific primers in mouse glomeruli isolated from non-
644 transplanted -/- mice (black bar, 0), transplanted +/+ mice (red bars) and
645 transplanted -/- mice (blue bars) mice. *** $P < 0.001$, $n = 8$ animals per group,
646 error bars are SEM. Values were normalised to total β -actin using mouse-

647 human non-specific primers ($2^{-\Delta\text{CT}}$). **B.** Immunohistochemistry showing
648 human-specific vimentin staining (brown) in the glomeruli of non-transplanted
649 and transplanted $-/-$ mice (counterstained with haematoxyllin), **and human-**
650 **specific podocin in non-transplanted $-/-$ mice.** X200, X400 and x40
651 magnifications. **C.** Quantitative real-time RT-PCR showing expression of
652 podocyte markers (CR1, VEGFA, SYNAPTOPODIN, CD2AP) using human-
653 specific primers that do not amplify mouse sequences in CSC (black bars),
654 and in the glomeruli of transplanted (green bars), non-transplanted (red
655 values) $-/-$ mice **and in $+/+$ mice (blue values).** Values were normalised to
656 human-specific β -actin (ΔCT). $n=8$ per group, error bars are SEM. **D.**
657 Western blot showing detection of human-specific PODOCIN, **CD2AP** and
658 COL4A3 protein within the glomeruli of transplanted and non-transplanted $-/-$
659 mice, **and non-transplanted $+/+$ mice.** GAPDH was used as loading control.
660 **E.** Immunofluorescence for COL4A3 in kidneys of non-transplanted and
661 transplanted $-/-$ mice. Scale bar = 25 and 10 μm .

662

663 **Figure 3 | CSC transplantation prevented weight loss in $-/-$ mice and**
664 **reduced levels of blood urea and cortical fibrosis.** **A.** Percentage of 9
665 week-old transplanted and non-transplanted $-/-$ mice ($n= 48$ and 25 ,
666 respectively) showing a weight loss above (white box, mice alive) or below
667 (black box, mice culled before the age of 9 weeks) the 20% required for the
668 Home Office to maintain mice alive (top graph). **B.** Weight of 9 week-old non-
669 transplanted $+/+$ ($n=15$, red bars), non-transplanted $-/-$ ($n=10$, blue bars) and
670 transplanted $-/-$ mice ($n=8$ per group, green bars), error bars are SEM. *
671 $P<0.05$. **C.** Blood urea levels (mmol/L) in non-transplanted $+/+$ (upper panel,

672 red dots, n=41) and -/- mice (middle panel, blue dots, n=45) measured over
673 90 days. **D.** Blood urea levels in 9 week-old non-transplanted +/+ mice (red
674 dots, n=10), non-transplanted -/- mice (blue dots, n=10), and CSC-
675 transplanted -/- mice (green dots, n=25). Bars are mean and SEM. ***
676 $P < 0.001$. **E. Urine proteinuria levels (albumin / creatinine ratios) in 9 week-old**
677 **non-transplanted +/+ mice (red dots, n=21), non-transplanted -/- mice (blue**
678 **dots, n=16), and CSC-transplanted -/- mice (green dots, n=21). Bars are**
679 **mean and SEM. ** $P < 0.01$.**

680

681 **Figure 4 | CSC transplantation reduced cortical inflammation in -/-**
682 **glomeruli. A.** Quantification of picrosirius red staining (PSR) within the renal
683 cortical area of non-transplanted (blue bar) and transplanted (green bar) -/-
684 mice, two weeks after transplantation. *** $P < 0.0001$, n=4 animals per group.
685 5 independent fields were quantified per sample, data are expressed as area
686 sum. **B.** Polarised images of kidney sections from non-transplanted and
687 transplanted -/- mice, stained with picrosirius red. Scale bar 200 μ m. **C.**
688 Quantification of CD4, CD68 and CD45.2-positive staining within the cortical
689 area of non-transplanted (blue bars) and transplanted (red bars) -/- mice. ***
690 $P < 0.001$, n=4 animals per group, error bars are SEM. 5 independent fields
691 were quantified per sample, data are expressed as area sum. **D.**
692 Immunohistochemistry for mouse-specific anti-CD4, CD68 and CD45.2
693 (brown) in the glomeruli of 9 week-old transplanted and non-transplanted -/-
694 mice (counterstained in blue). X200 magnification.

695

696 **Figure 5 | Expression of endogenous murine renal markers is modulated**
697 **by CSC transplantation.** Quantitative real-time RT-PCR showing expression
698 of podocyte markers using mouse-specific primers that do not amplify human
699 sequences (*Nephrin*, *Podocin*, *Vegfa*, *Synaptopodin*, *Cd2ap*, *Cr1*), in the
700 glomeruli of non-transplanted +/+ mice (red bars), non-transplanted -/- mice
701 (black bars), and transplanted -/- mice (white bars). Values were normalised
702 to mouse-specific cyclophilin. –*** P<0.001, *P<0.05, n=8 per group, error
703 bars are SEM.

704

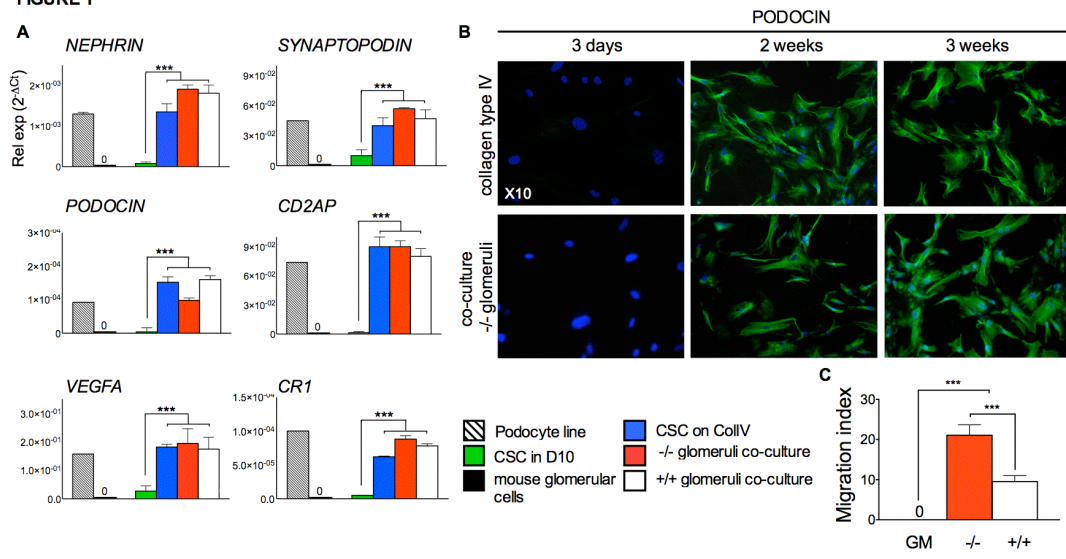
705 **Table 1**

706 List of primers used for RT-PCR and real-time RT-PCR

707

708

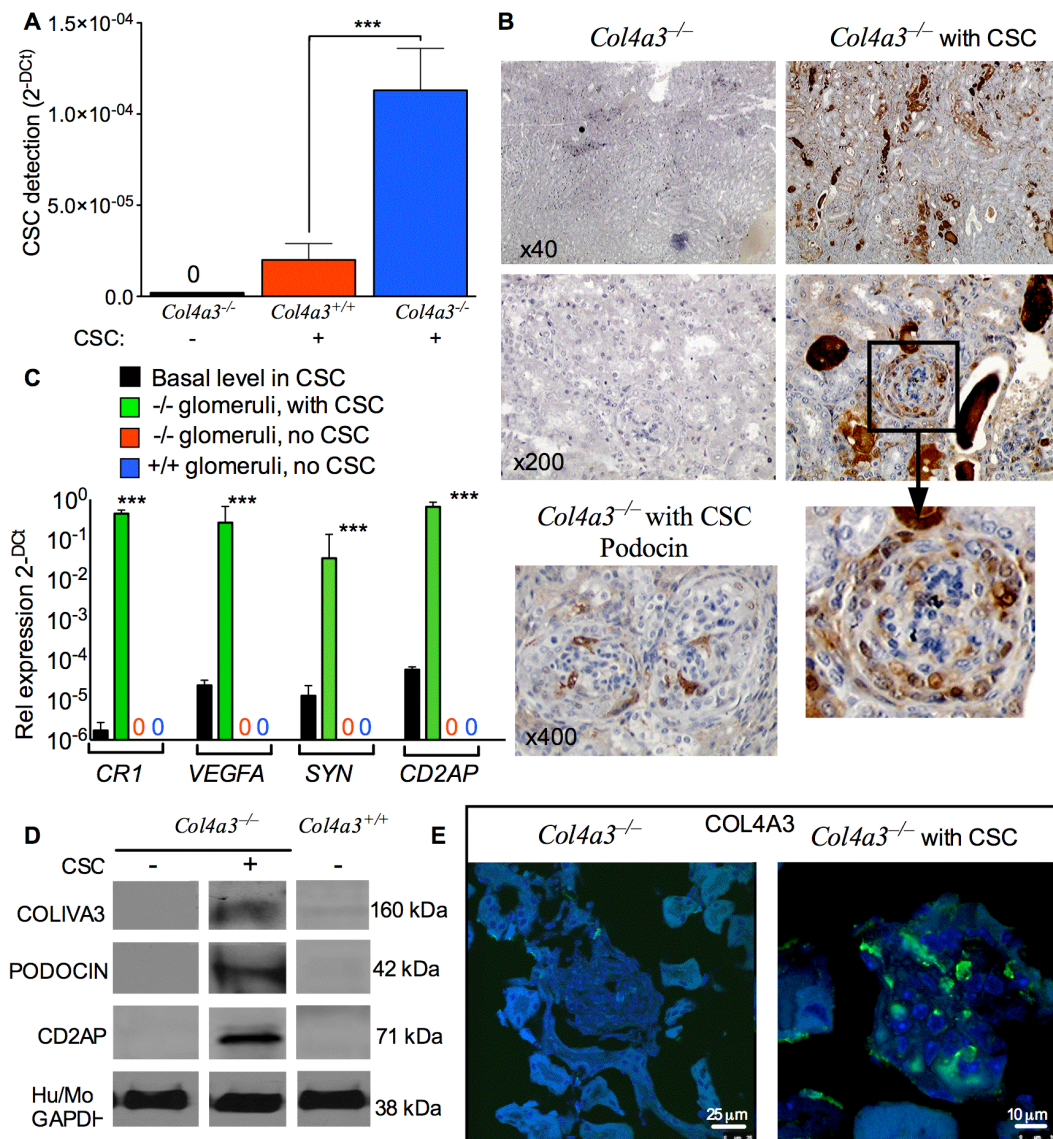
FIGURE 1



709

710

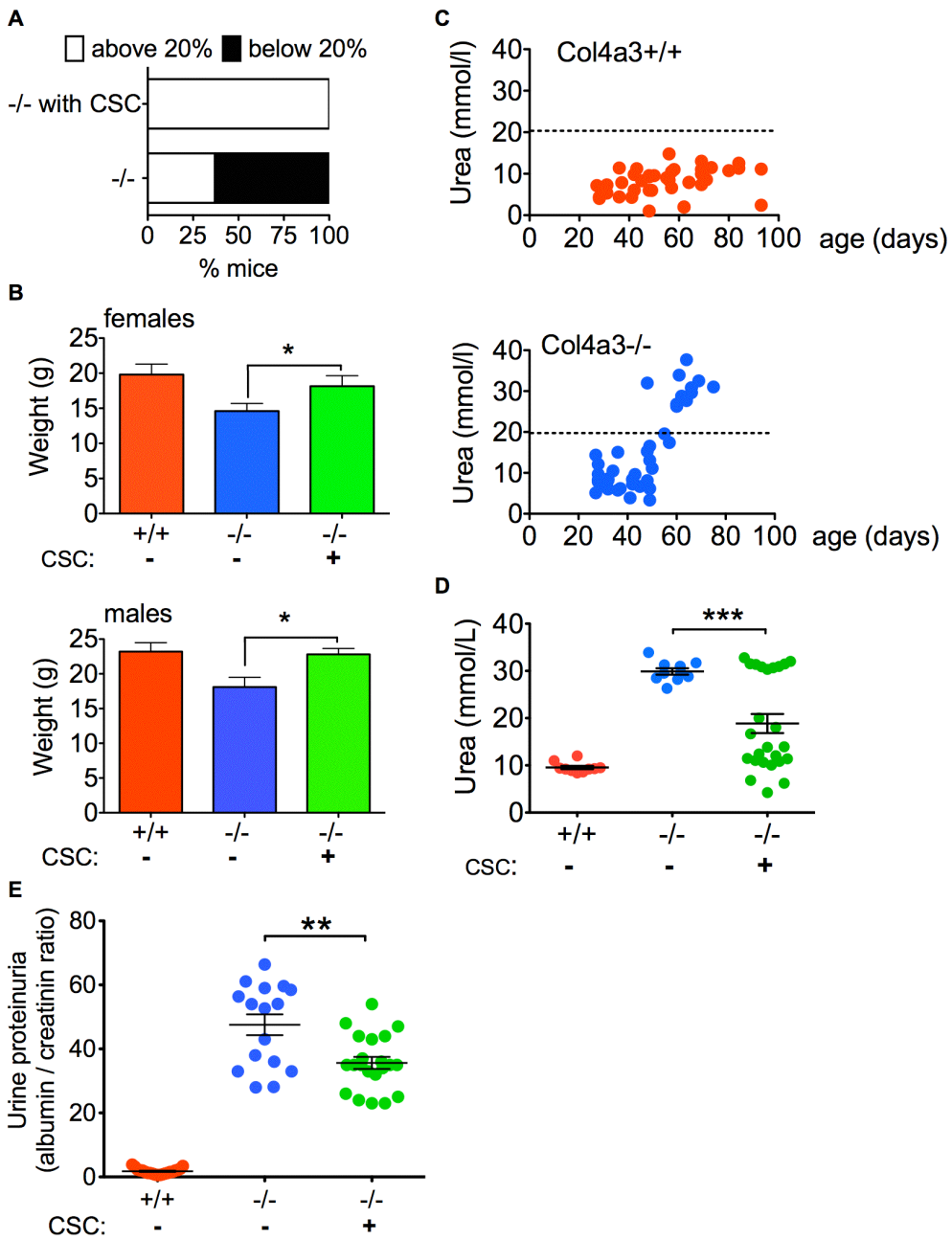
FIGURE 2



711

712

FIGURE 3

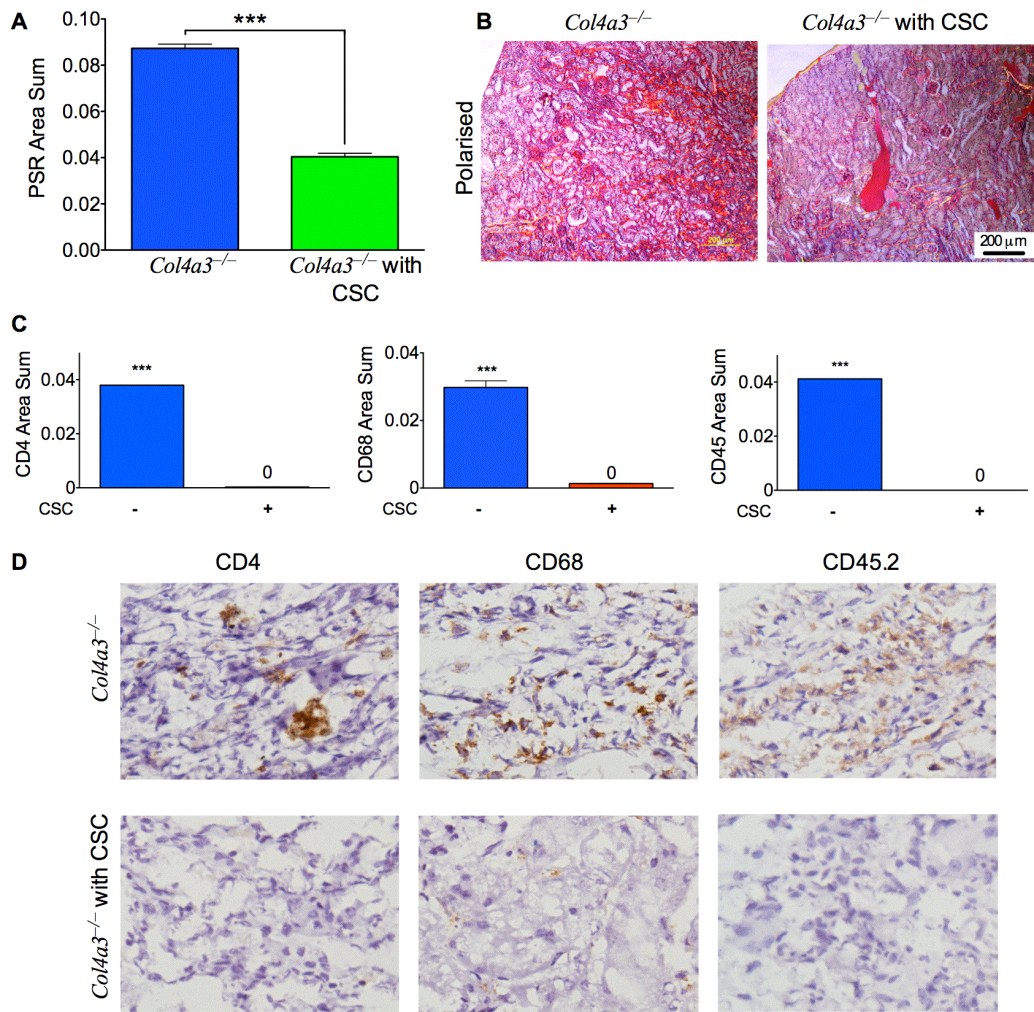


713

714

715

FIGURE 4

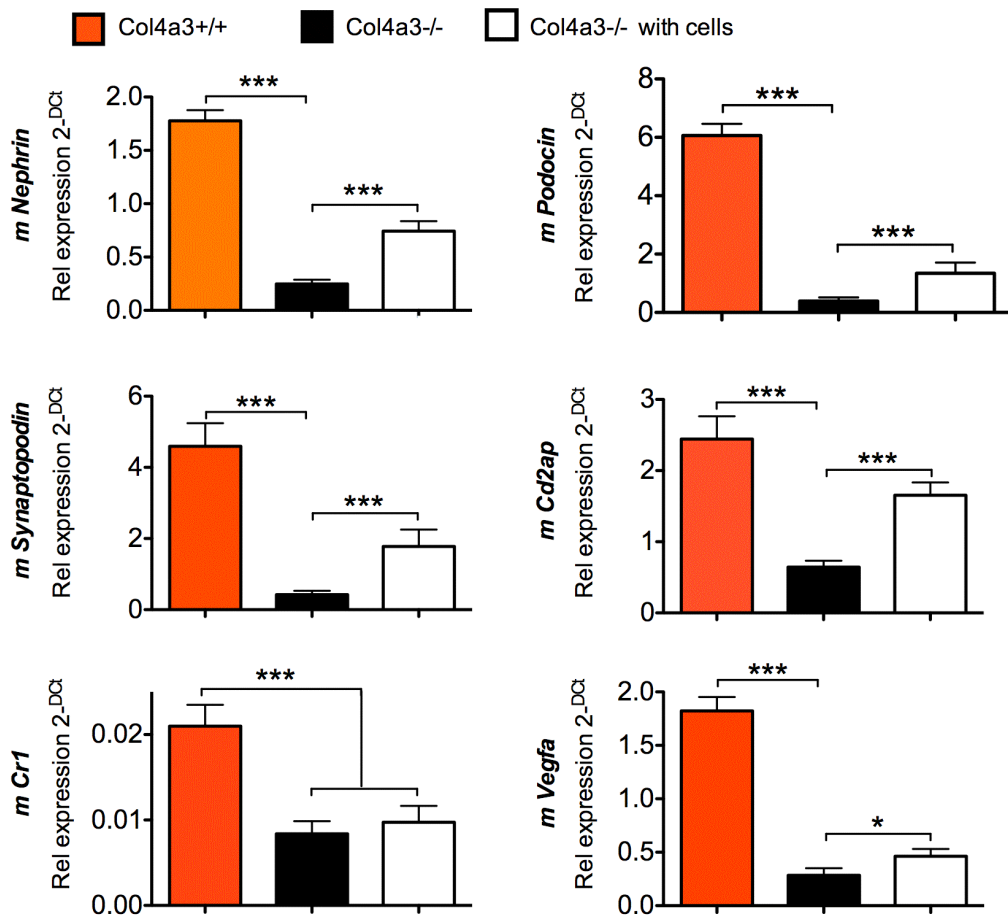


716

717

718

FIGURE 5



719

720

721

Table 1

Gene	Accession no.	Primers (5'→3')
BMI1	NM_005180	F: CTGGTTGCCCATGACAGC
		R: CAGAAAATGAATGCGAGCCA
NEPHRIN	NM_004646	F: CTCTGGAACCCGATTCTCTG
		R: TGGGTTTTATGGAGCTGACC
SYNAPTOPODIN	NM_007286	F: GGAGGATGATGGGGCAGC
		R: GGGTCGGAGCTGGGATAC
PODOCIN	NM_014625	F: TGGGGAATCAAAGTGGAGAG
		R: GAATCTCAGCTGCCATCCTC
CD2AP	NM_012120	F: CACATCCACAAACCAAAAACATT
		R: CTCCACCAGCCTTCTTCTACC
VEGF-A	NM_001025366	F: TCCTCACACCATTGAAACCA
		R: TTTTCTCTGCCTCCACAATG
CR1	NM_000651	F: TGGCATGGTGCATGTGATCA
		R: TCAGGGCCTGGCACTTCACA

722
723

724

725